Contents lists available at ScienceDirect

Immunobiology

journal homepage: http://ees.elsevier.com

Epigenetics in non-classical monocytes support their pro-inflammatory gene expression

Lu Zhang [a], Thomas P. Hofer [b], Adam M. Zawada [c], Björn Rotter [d], Nicolas Krezdorn [d], Elfriede Noessner [b], Yvan Devaux [a], Gunnar Heine [c], Loems Ziegler-Heitbrock [e,*]

[a] Cardiovascular Research Unit, Luxembourg Institute of Health, Luxembourg
[b] Immunoanalytics Research Group Tissue Control of Immunocytes, Helmholtz Center Munich, Munich, Germany
[c] Department of Internal Medicine IV, Saarland University Medical Center, Homburg, Germany
[d] GenXPro GmbH, Frankfurt/Main, Germany
[e] Monocytomics Research, Herrsching, Germany

ARTICLE INFO

ABSTRACT

Non-classical human monocytes are characterized by high-level expression of cytokines like TNF, but the mechanisms involved are elusive. We have identified miRNAs and CpG-methylation sites that are unique to non-classical monocytes, defined via CD14 and CD16 expression levels. For down-regulated miRNAs that are linked to up-regulated mRNAs the dominant gene ontology term was intracellular signal transduction. This included down-regulated miRNA-20a-5p and miRNA-106b-5p, which both are linked to increased mRNA for the TRIM8 signaling molecule. Methylation analysis revealed 16 hypo-methylated CpG sites upstream of 14 differentially increased mRNAs including 2 sites upstream of TRIM8. Consistent with a positive role in signal transduction, high TRIM8 levels went along with high basal TNF mRNA levels in non-classical monocytes. Since cytokine expression levels in monocytes strongly increase after stimulation with toll-like-receptor ligands, we have analyzed non-classical monocytes (defined via slan expression) after stimulation with lipopolysaccharide (LPS). LPS-stimulated cells continued to have low miRNA-20a and miRNA-106b and high TRIM8 mRNA levels and they showed a 10-fold increase in TNF mRNA. These data suggest that decreased miRNAs and CpG hypo-methylation is linked to enhanced expression of TRIM8 and that this can contribute to the increased TNF levels in non-classical human monocytes.

1. Introduction

Monocyte subsets have been described based on flow cytometry studies using monoclonal antibodies against human CD14 and CD16 (Passlick et al., 1989). The CD16-positive cells compared to the CD16-negative monocytes were shown to have pro-inflammatory features such as the production of high levels of the pro-inflammatory cytokine TNF and low levels of the anti-inflammatory cytokine IL-10 (Frankenberger et al., 1996; Belge et al., 2002). These cells can dramatically increase in number in inflammatory disease (Fingerle et al., 1993) and conversely their numbers are selectively depleted by treatment with anti-inflammatory glucocorticoids (Fingerle-Rowson et al., 1998; Dayyani et al., 2003). While initially two types of blood monocytes were defined, more recently it emerged that an intermediate type of monocytes with high CD14 and low CD16 can be delineated (Ziegler-Heitbrock et al., 2010) such that now three subsets termed classical, intermediate and non-classical monocytes are recognized. The intermediate cells were shown to have highest MHC class II expression (Zawada et al., 2011; Wong et al., 2012) and to have prognostic value with respect to cardiovascular events in at risk populations (Rogacev et al., 2012). For the dissection of this intermediate CD14++CD16+ monocytes and the non-classical monocytes based on the expression level of CD14 different approaches were taken (Zawada et al., 2015). In order to circumvent the problem of having to define a cut-off in the continuous level of CD14 expression it was proposed to use additional markers like slan to positively identify the non-classical monocytes and separate them from intermediate monocytes (Wong et al., 2011). In fact, it could be demonstrated that this marker is able to unequivocally define non-classical monocytes and that this definition is informative in inflammatory disease (Hofer et al., 2015). Also for slan-positive monocytes it had been shown earlier that these cells are superb producers of pro-inflammatory cytokines (Schakel et al., 2002; Dutertre et al., 2012). Still, the mechanisms responsible for the increased cytokine production remained elusive. We now have determined the epigenetic features of the non-classical monocytes by

Abbreviations: LPS, lipopolysaccharide; slan, 6-sulfo LacNAc; TNF, tumor necrosis factor; TRIM8, tripartite motif containing 8.

* Corresponding author.
E-mail address: LZH@monocyte.eu (L. Ziegler-Heitbrock)

https://doi.org/10.1016/j.imbio.2020.151958
Received 29 April 2020; Accepted 5 May 2020
Available online xxx
0171-2985/

identification of miRNAs and of hypo-methylated sites that are unique to these cells compared to both classical and intermediate monocytes. Our data show that a majority of the down-regulated miRNAs is linked to intracellular signaling processes and that the upregulated TRIM8 is the target of two downregulated miRNAs and carries two up-stream hypo-methylated CpG sites. Low miRNA-20a and 106b and high TRIM8 and TNF are found in non-classical monocytes defined via CD14 and CD16, and also via slan, and this was also true after LPS stimulation of slan-defined non-classical monocytes.

2. Material and methods

2.1. Isolation of monocyte subsets for RNA expression and DNA methylation analyses

This is a reanalysis of data sets published before (Zawada et al., 2017; Zawada et al., 2016; Hofer et al., 2015). The detailed description of monocyte isolation is provided in these publications. In brief, monocyte subsets were isolated with MACS technology. Initially NK cells and neutrophils were depleted from peripheral blood mononuclear cells by using the Non-monocyte Depletion Cocktail (CD16+ Monocyte Isolation Kit, Miltenyi Biotec) followed by separation of classical and intermediate monocytes from non-classical monocytes by using anti-CD14 FITC antibody (clone TÜK 4, Miltenyi Biotec) and anti-FITC MultiSort MicroBeads (Anti-FITC MultiSort Kit; Miltenyi Biotec). Finally, classical and intermediate monocytes, as well as non-classical monocytes and non-monocytes, were separated with CD16 microbeads. Representative dot plots of isolated monocyte subsets are depicted as insets in Fig. 1.

All participants recruited for this study gave informed consent. The study protocol was approved by the local Ethics Committee.

2.2. Isolation and culture of monocyte subsets for validation

For isolation of monocyte subsets, peripheral blood mononuclear cells (PBMC) were prepared from 100 mL heparinized blood obtained from healthy volunteers by Ficoll (Biocoll, #L6115, Biochrom, Berlin, Germany) density gradient separation.

Monocytes were isolated by no-touch procedures from PBMC using the MACS Pan Monocyte Isolation Kit (#130-096-537, Miltenyi, Bergisch Gladbach, Germany) according to the manufacturer's instructions. In brief, PBMC were incubated with the non-monocyte depletion cocktail of biotin-labelled antibodies with subsequent incubation with anti-biotin microbeads. Labelled cell suspension was run over two sequential LS columns and flow-through was collected representing the enriched monocytes.

The cells were then incubated with anti-slan FITC-labelled antibodies (#130-093-027, Miltenyi, Bergisch Gladbach, Germany) and subsequently incubated with magnetic bead-labelled anti-FITC antibodies (anti-FITC Multi Sort Kit #130-058-701, Miltenyi, Bergisch Gladbach, Germany).

Cells were run over a LS column; slan-negative cells from the flow-through were collected and slan-positive cells were eluted from the column and subsequently incubated with Multi Sort Release agent (#130-058-701) to release the magnetic beads from the antibodies and run over an additional LS column to remove all remaining magnetic beads.

Then both slan-negative and slan-positive cell populations were incubated with magnetic bead-labelled anti-CD16 antibodies (#130-.045-701, Miltenyi, Bergisch Gladbach, Germany) and subsequently run over three MS columns. Flow through of the CD16-treated slan-negative population represents slan -negative CD16-negative CD14-positive classical monocytes and the eluted cells from the CD16-treated slan-positive population represent slan -positive CD16-positive CD14-positive non-classical monocytes. Cell populations were analyzed by flow cytometry and were used when purity was >91%.

Classical monocytes and slan-positive non-classical monocytes were treated with or without 10 ng of LPS /mL (#581-009-L002 S. abortus equi ultra pure, Alexis, Lausen, Switzerland) at 1–3 × 10E6/mL for 2 h. Then, cells were washed once with PBS, lysed in an appropriate amount of QIAzol (#79306, Qiagen, Hilden, Germany) and stored at −20 °C until further processing.

2.3. Next generation sequencing

MACE (Massive analysis of complementary DNA ends) analysis for the determination of gene expression is described in Hofer et al. (2015), small RNA-seq analysis for the determination of miRNA expression is described in Zawada et al. (2017), and methyl-Seq analysis for the determination of DNA methylation is described in Zawada et al. (2016).

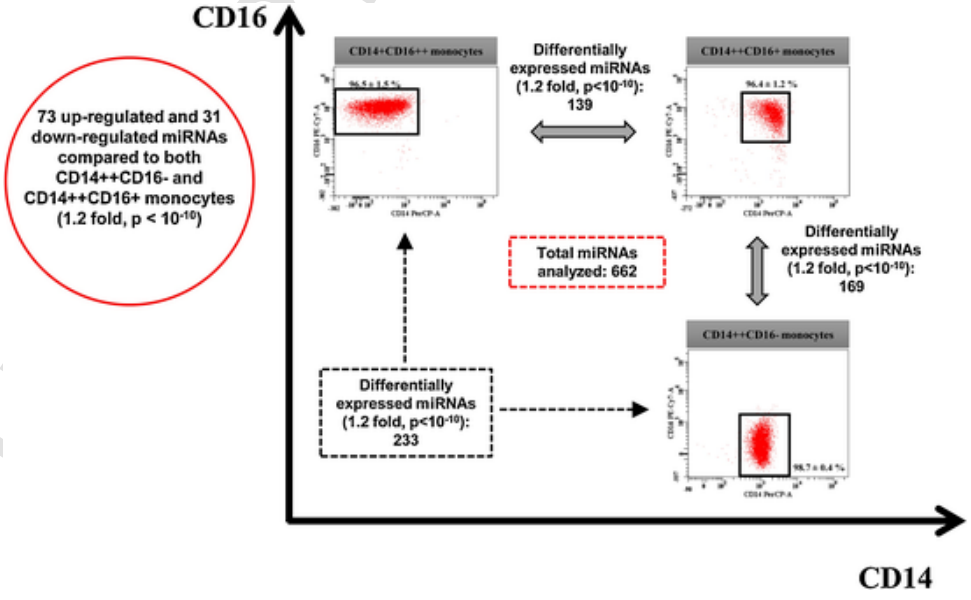

Fig. 1. Monocyte subsets isolated based on CD14 and CD16 expression: overview of differential miRNAs. Monocyte subsets were isolated using MACS technology based on differential expression of CD14 and CD16 as described (Zawada et al., 2011).

In brief, for MACE analysis ten barcoded samples were sequenced simultaneously after generation of MACE libraries consisting of poly-adenylated 3′ mRNA ends in one lane of a HiSeq 2000 machine (Illumina, San Diego, CA) with 1 × 100 bp. MACE reads were polyA-trimmed, and the quality region was removed. Mapping of reads to the human genome (hg19) was performed with NovoAlign (http://novocraft.com). The statistical programming language R (www.r-project.org) with the DESeq package (Anders and Huber, 2010) was used for normalization and testing for differential expression. Expression levels are given in tags per million (TPM).

For small-RNA-seq, the miRNA population with flanking p5 and p7 adapters was also sequenced on a Hiseq2000 machine. The analysis of the small RNA-Seq libraries was performed using omiRas (http://tools.genxpro.net/omiras) (Muller et al., 2013). The differential expression analysis was done with the DEGseq Bioconductor package (Wang et al., 2010).

For Methyl-Seq analysis, we used the restriction enzyme HpaII. The fractions were ligated with "TrueQuant" Y-adapters (GenXPro) and adapters containing Illumina P7 priming sites. The products were PCR amplified using P5 and P7 primers with 10 cycles and sequenced on the Hiseq2000 machine. Reads were quality-trimmed and mapped to the human genome (hg19) using novoalign (http://www.novocraft.com/products/novoalign/). The RefSeq track, as well as the CpG island track from the UCSC table browser (https://genome.ucsc.edu/cgi-bin/hgTables), were used to annotate genomic restriction sites. Regions up to 2 kb upstream of the transcription start site (TSS) of genes contained in the RefSeq track were defined as promoter regions. To test for differential methylation, quantification results for all restriction sites were normalized to tags per million (NML) and a statistical test was carried out using NOISeq (Tarazona et al., 2011).

2.4. Characterization of differentially expressed miRNAs

As described before (Zawada et al., 2017), analysis of biological processes for differentially expressed miRNAs was performed using DIANA-miRPath v3.0 (Vlachos et al., 2015) implemented with miRNA targets from DIANA microT-CDS (Paraskevopoulou et al., 2013). The significance level (p-value) of biological process terms was adjusted with Bonferroni correction as described elsewhere (Hochberg, 1988). Only the terms with Bonferroni corrected p value < 0.05 were accounted for significance. Biological process level was defined as the depth of node in AmiGO2 inferred tree view (Carbon et al., 2009). The depth of biological process was set to 0 and those terms deeper than 4 were considered relevant. Child annotation terms were discarded to avoid redundancy. miRNAs and biological process terms were clustered according to the significance level (p-value) between each miRNA and term using Euclidean distance integrated into Cluster3.0 (de Hoon et al., 2004). Heatmaps were generated with Java TreeView (Saldanha, 2004).

2.5. Interaction of differentially expressed miRNAs and mRNAs

DIANA microT-CDS was used to obtained interaction between differentially expressed miRNAs and mRNAs ($p < 10^{-10}$ & fold-change ≥ 1.2). Interaction network was generated using Cytoscape (Shannon et al., 2003). Functional enrichment analysis of mRNAs in the network was performed with DAVID (Huang da et al., 2009). Biological processes with FDR $< 5\%$ were considered significantly enriched terms.

2.6. Total RNA extraction and quantitative RT-PCR

The cell pellet was homogenized in QIAzol Lysis Reagent (Qiagen). Cell lysates were stored at –80 °C before RNA extraction. Total RNA was extracted using the miRNeasy® Micro kit (Qiagen). After extraction, RNA was quantified with the ND-1000 spectrophotometer (NanoDrop® Technologies). Total RNA was reverse-transcribed using the miScript II RT kit (Qiagen). Real-time PCR was performed in a CFX96 apparatus (Biorad) with IQ SYBR Green Supermix (Biorad). The primers of mRNAs were designed with the Beacon Designer software (Premier Biosoft; Table S1). For mature miRNA quantification we used the miScript Primer Assay (Qiagen), with the primer sequences not being disclosed by the provider. Splicing factor 3a subunit 1 (SF3A1) and RNA U6 small nuclear 2 (RNU6-2) were chosen as housekeeping genes for normalization of mRNA and miRNA, respectively. Expression levels were calculated by the relative quantification method (ΔΔCt) using the CFX Manager 2.1 (Bio-Rad).

2.7. Statistics

The SigmaPlot v12.5 software was used for statistical analyses. Comparisons between two groups were performed using a two-tailed Student's test. Results are presented as a mean ± standard deviation. A p-value < 0.05 was considered significant.

3. Results

3.1. Differential expression of miRNAs in non-classical monocytes

Initially, we isolated three human monocyte subsets based on the differential expression of CD14 and CD16 and generated miRNA libraries as described in detail earlier (see Zawada et al., 2017). The total of 662 miRNA, which had been determined by RNAseq, was analyzed in the present study for differential expression in non-classical monocytes as compared to both intermediate and classical monocytes. With a cut-off of 1.2 fold, we found 31 miRNAs decreased and 73 miRNAs increased in the non-classical monocytes (see Fig. 1).

Table 1 is a compilation of the total of 92 miRNAs with an at least two-fold difference between non-classical monocytes and either intermediate or classical monocytes. The fold-change was up to 969-fold compared to classical monocytes (hsa-miRNA-493-5p, $\log_2$ fold change = 9.92) and up to 60-fold compared to intermediate monocytes (hsa-miRNA-876-5p, log2 fold change = 5.90) (see Table 1).

Two miRNAs (hsa-miR-655 and hsa-miR-876-5p) were almost exclusively expressed by the non-classical monocytes.

In analyzing the biological processes associated with these unique miRNAs, we found 27 of 31 down-regulated miRNAs to be significantly ($p < 0.05$) associated with 13 biological processes (Bonferroni adjusted $p < 0.05$ and level > 4) (see Fig. 2A). Of note, six of these 13 processes involve signaling.

When looking at the biological processes associated with up-regulated miRNAs we found 64 of the 73 miRNAs to be significantly ($p < 0.05$) associated with 35 biological processes (Bonferroni adjusted $p < 0.05$ and level > 4). As shown in Fig. 2B, ten of these biological processes represent signaling pathways.

The top up-regulated miRNA (miR 493-5p; almost 1000-fold increase in non-classical compared to classical monocytes) was associated with seven biological processes that involve signaling.

Many of the biological processes targeted by up-regulated miRNAs ($n = 12$) were also targeted by down-regulated miRNAs (see* in Fig. 2A and B) and six of these involve signaling.

3.2. Interaction between differentially expressed miRNAs and mRNAs in non-classical monocytes

The uniquely decreased miRNAs in non-classical monocytes were then tested for interaction with the uniquely up-regulated mRNAs in these cells and vice versa. Twenty-seven of the down-regulated miRNAs interacted with 194 up-regulated mRNAs as depicted in Figure S1A.

Table 1
Differential miRNAs in non-classical monocytes.

ID	TPM			p-value CD14 + CD16 + + non-classical monocytes versus		log2FC CD14 + CD16 + + non-classical monocytes versus	
	CD14 + + CD16-	CD14 + + CD16 +	CD14 + CD16 + +	CD14 + + CD16-	CD14 + + CD16 +	CD14 + + CD16-	CD14 + + CD16 +
hsa-miR-493-5p#	0.0	43.1	186.7	1.60E−104	6.51E−71	9.92	2.11
hsa-miR-369-3p#	0.0	28.9	176.9	3.31E−100	5.98E−86	9.84	2.61
hsa-miR-495-3p	0.0	33.2	175.1	1.92E−99	2.31E−77	9.83	2.40
hsa-miR-432-5p	0.0	19.4	125.3	1.69E−76	2.32E−63	9.34	2.69
hsa-miR-494	0.0	28.9	111.3	1.26E−69	9.37E−39	9.17	1.94
hsa-miR-136-3p	0.0	29.7	101.6	8.44E−65	1.29E−31	9.04	1.78
hsa-miR-134	0.0	21.4	93.5	1.26E−60	1.05E−36	8.92	2.13
hsa-miR-382-5p	0.0	12.7	74.5	1.58E−50	2.23E−36	8.59	2.56
hsa-miR-127-5p	0.0	24.1	68.3	4.03E−47	1.84E−17	8.47	1.50
hsa-miR-409-3p	0.8	65.7	247.4	2.88E−168	3.43E−82	8.33	1.91
hsa-miR-376a-3p	0.0	9.1	57.7	4.34E−41	8.10E−30	8.23	2.66
hsa-miR-493-3p	0.0	13.1	57.7	4.34E−41	1.73E−23	8.23	2.14
hsa-miR-376c-3p	0.0	11.5	56.2	3.15E−40	9.18E−25	8.19	2.29
hsa-miR-154-3p	0.0	11.9	55.8	6.11E−40	8.19E−24	8.18	2.23
hsa-miR-337-3p	0.0	11.1	40.7	7.55E−31	1.48E−14	7.72	1.88
hsa-miR-379-5p	0.8	31.3	160.1	2.49E−116	1.74E−69	7.70	2.36
hsa-miR-758-3p	0.0	13.1	39.0	9.21E−30	2.73E−11	7.66	1.58
hsa-miR-654-3p	0.8	45.5	150.7	1.96E−110	2.16E−44	7.61	1.73
hsa-miR-487b	0.8	25.3	145.5	3.81E−107	2.24E−68	7.56	2.52
hsa-miR-485-5p	0.0	6.3	36.3	4.92E−28	2.97E−18	7.55	2.52
hsa-miR-431-5p	0.0	9.1	33.8	1.93E−26	1.85E−12	7.45	1.89
hsa-miR-127-3p	5.0	259.7	835.8	0.00E + 00	7.73E−230	7.38	1.69
hsa-miR-411-5p	0.0	5.1	31.3	8.02E−25	1.51E−16	7.34	2.61
hsa-miR-299-3p	0.0	8.3	29.8	7.72E−24	7.63E−11	7.27	1.84
hsa-miR-654-5p	0.0	3.6	26.6	1.13E−21	7.96E−16	7.11	2.90
hsa-miR-370	0.0	3.6	25.4	7.90E−21	7.70E−15	7.04	2.83
hsa-miR-381-3p	1.2	45.1	151.2	1.63E−115	3.93E−45	7.03	1.74
hsa-miR-543	1.9	40.8	250.1	6.93E−190	6.42E−121	7.02	2.62
hsa-miR-485-3p	0.8	26.1	85.8	2.92E−67	8.56E−26	6.80	1.72
hsa-miR-889	0.0	3.2	21.0	1.03E−17	4.48E−12	6.76	2.73
hsa-miR-154-5p	1.2	40.0	112.0	5.27E−88	3.16E−27	6.60	1.49
hsa-miR-655 §	0.0	0.8	18.0	1.43E−15	6.87E−15	6.55	4.51
hsa-miR-431-3p	0.0	2.0	17.0	7.62E−15	2.95E−11	6.46	3.10
hsa-miR-433	0.0	0.8	16.3	2.71E−14	2.01E−13	6.40	4.36
hsa-miR-876-5p §	0.0	0.0	11.8	6.83E−11	8.42E−11	5.94	5.90
hsa-miR-342-5p	30.5	420.0	733.9	0.00E + 00	7.13E−64	4.59	0.81
hsa-miR-146a-5p	754.4	5027.8	16045.0	0.00E + 00	0.00E + 00	4.41	1.67
hsa-miR-132-5p	2.7	21.4	56.2	5.81E−43	2.73E−13	4.38	1.40
hsa-miR-1301	29.3	380.8	515.1	0.00E + 00	3.47E−16	4.14	0.44
hsa-miR-132-3p	52.8	454.4	889.5	0.00E + 00	1.06E−104	4.07	0.97
hsa-miR-181d	57.9	158.3	383.8	7.17E−195	3.75E−71	2.73	1.28
hsa-miR-505-5p	10.4	21.4	62.9	9.05E−32	5.13E−17	2.59	1.56
hsa-let-7b-5p	6301.3	25077.6	35476.4	0.00E + 00	0.00E + 00	2.49	0.50
hsa-miR-378i	23.5	52.2	123.6	1.45E−55	4.20E−23	2.39	1.24
hsa-miR-185-3p	89.5	551.8	427.0	1.43E−174	4.32E−13	2.25	−0.37
hsa-miR-29b-2-5p	155.0	437.8	684.1	2.39E−261	6.47E−41	2.14	0.64
hsa-miR-342-3p	2191.8	5141.4	9393.3	0.00E + 00	0.00E + 00	2.10	0.87
hsa-miR-1249	125.3	648.0	519.3	2.60E−188	7.84E−12	2.05	−0.32
hsa-miR-744-5p	654.5	3122.7	2605.5	0.00E + 00	2.02E−35	1.99	−0.26
hsa-miR-29b-3p	391.5	982.0	1358.5	0.00E + 00	1.79E−45	1.80	0.47
hsa-miR-29c-5p	345.2	935.3	1195.7	0.00E + 00	1.21E−24	1.79	0.35

Table 1 (*Continued*)

ID	TPM			p-value CD14 + CD16 + + non-classical monocytes versus		log2FC CD14 + CD16 + + non-classical monocytes versus	
	CD14 + + CD16-	CD14 + + CD16 +	CD14 + CD16 + +	CD14 + + CD16-	CD14 + + CD16 +	CD14 + + CD16-	CD14 + + CD16 +
hsa-let-7d-3p	269.2	1163.7	854.3	3.42E−233	5.39E−36	1.67	−0.45
hsa-miR-197-3p	639.9	1691.0	2011.0	0.00E + 00	1.24E−21	1.65	0.25
hsa-miR-29c-3p	1196.0	2589.1	3392.2	0.00E + 00	1.34E−79	1.50	0.39
hsa-miR-326	100.7	344.4	257.0	4.96E−53	9.74E−11	1.35	−0.42
hsa-miR-3613-5p	288.5	882.3	733.4	8.70E−147	1.74E−11	1.35	−0.27
hsa-miR-34a-5p	199.4	389.1	506.4	8.22E−102	1.04E−12	1.34	0.38
hsa-miR-423-3p	1737.1	4654.9	4194.9	0.00E + 00	6.04E−19	1.27	−0.15
hsa-miR-378a-3p	4334.3	7227.0	10447.6	0.00E + 00	0.00E + 00	1.27	0.53
hsa-let-7c	531.9	960.7	1271.4	6.94E−228	6.01E−33	1.26	0.40
hsa-miR-181c-5p	203.3	222.1	475.9	2.44E−83	1.51E−69	1.23	1.10
hsa-let-7g-5p	17569.1	27785.4	37095.4	0.00E + 00	0.00E + 00	1.08	0.42
hsa-miR-27a-3p	9439.6	15976.3	19657.4	0.00E + 00	1.91E−279	1.06	0.30
hsa-miR-28-3p	877.8	1257.5	1825.7	1.28E−247	1.93E−77	1.06	0.54
hsa-miR-708-5p	141.2	167.8	293.3	3.12E−41	1.46E−26	1.06	0.81
hsa-miR-361-3p	462.4	658.3	945.1	3.89E−124	8.08E−39	1.03	0.52
hsa-miR-378c	204.8	243.8	415.9	6.87E−55	2.30E−34	1.02	0.77
hsa-miR-33a-5p	128.0	500.3	225.2	2.38E−21	1.63E−78	0.81	−1.15
hsa-miR-223-3p	64733.8	51265.0	31958.2	0.00E + 00	0.00E + 00	−1.02	−0.68
hsa-miR-450a-5p	605.9	524.5	298.7	6.72E−79	8.61E−47	−1.02	−0.81
hsa-miR-503-5p	262.7	209.8	125.6	1.25E−37	4.96E−17	−1.06	−0.74
hsa-miR-17-5p	7930.8	4334.3	3523.4	0.00E + 00	3.59E−62	−1.17	−0.30
hsa-miR-301a-3p	937.6	531.6	410.2	3.12E−155	6.76E−13	−1.19	−0.37
hsa-miR-19b-3p	24163.6	16996.4	10553.5	0.00E + 00	0.00E + 00	−1.20	−0.69
hsa-miR-19a-3p	9747.0	7930.8	4150.0	0.00E + 00	0.00E + 00	−1.23	−0.93
hsa-miR-199b-5p	482.9	340.8	205.2	2.74E−85	3.73E−26	−1.23	−0.73
hsa-miR-221-3p	5148.9	3927.8	2146.7	0.00E + 00	0.00E + 00	−1.26	−0.87
hsa-miR-223-5p	2942.0	1485.5	1216.2	0.00E + 00	4.76E−21	−1.27	−0.29
hsa-miR-222-3p	3280.6	1919.0	1261.1	0.00E + 00	2.99E−100	−1.38	−0.61
hsa-miR-106b-5p $	15991.3	7701.6	6035.9	0.00E + 00	7.12E−148	−1.41	−0.35
hsa-miR-199a-3p	546.9	290.1	194.1	2.35E−128	2.03E−15	−1.49	−0.58
hsa-miR-20a-5p $	19398.8	10269.3	6304.8	0.00E + 00	0.00E + 00	−1.62	−0.70
hsa-miR-18a-5p	3516.3	1834.3	1080.2	0.00E + 00	2.19E−143	−1.70	−0.76
hsa-miR-148a-3p	1786.5	995.5	530.6	0.00E + 00	5.09E−105	−1.75	−0.91
hsa-miR-582-5p	280.8	176.9	80.2	3.53E−87	1.55E−28	−1.81	−1.14
hsa-miR-21-3p	734.7	327.3	208.4	1.59E−226	8.20E−21	−1.82	−0.65
hsa-miR-17-3p	619.8	347.5	171.7	2.58E−196	2.24E−45	−1.85	−1.02
hsa-miR-143-3p	288.5	137.0	78.0	8.32E−95	2.02E−13	−1.89	−0.81
hsa-miR-6503-5p §	62.1	45.5	16.5	4.58E−22	1.01E−11	−1.91	−1.46
hsa-miR-6503-3p #	177.0	102.9	43.2	7.09E−65	9.26E−20	−2.04	−1.25
hsa-miR-345-5p # §	1439.4	850.2	344.1	0.00E + 00	2.02E−160	−2.06	−1.30
hsa-miR-27a-5p #	859.7	361.0	192.9	0.00E + 00	5.72E−39	−2.16	−0.90

*Given are miRNAs that show an at least a 2-fold difference in non-classical monocytes compared to either classical or intermediates.
This covers 93 miRNAs of the entire set of 104 miRNA with an at least 1.2-fold difference.
= highest fold change compared to CD14 + + CD16- classical monocytes.
§ = highest fold change compared to CD14 + + CD16 + intermediate monocytes.
$ = miRNAs implicated in control of TRIM8.

Fig. 2. (A) Biological processes associated with miRNAs uniquely down-regulated in non-classical monocytes. For statistics see Table S2A, * = processes also associated with upregulated miRNAs as given in B. (B) Biological processes associated with miRNAs uniquely up-regulated in non-classical monocytes. For statistics see Table S2B, * = processes also associated with down-regulated miRNAs as given in A. The black line marks the association for the top miR 493-5p, which is increased 969-fold compared to classical monocytes.

Among these were interactions of miR-155-5p with the M-CSF-R cell surface receptor and miR148a-3p with the EMR1 receptor, the human homologue of the mouse F4/80 cell surface molecule. The top biological process for all of the upregulated mRNAs in this network was "intracellular signal transduction "(Table S2A). We therefore generated a network of these (n = 57) signaling-associated mRNAs together with the interacting miRNAs. As shown in Fig. 3A, signaling molecules that interact with down-regulated miRNAs included MAPK1, which is targeted by six miRNAs including the top down-regulated miRNA 345-5p, NCOA2, which is targeted by five miRNAs, and TRIM8, targeted by two miRNAs.

All of these molecules, together with a series of additional DEGs in this network, are enhancing signal transduction. This indicates that miRNAs may control the efficient signaling cascades in non-classical monocytes.

We then looked at the uniquely increased miRNA and the interaction with decreased mRNAs in non-classical monocytes. Here 69 up-regulated miRNAs interacted 160 down-regulated mRNAs (Figure S1B). This included interactions of miRNA 441-5p with the CD33 receptor and miR 185-5p with the CXCR4 receptor.

The top biological processes, enriched among the down-regulated mRNAs that interact with up-regulated miRNAs, involve „cell surface receptor signaling pathway "and „response to lipopolysaccharide ", which are related to "intracellular signal transduction, but the GO term „intracellular signal transduction" was not significant (FDR > 0.05, Table S3B). Since, however, this term was dominant among the up-mRNAs interacting with down-miRNA (see network in Fig. 3A, Table S3A) we generated an interaction map for the "intracellular signal transduction"- genes under this term also for the downregulated mRNAs. As shown in Fig. 3B, this map includes the top 4 up-regulated miRNAs and it shows the interactions of NFKBIA with 1 miRNA and of SOCS3 with 5 up-regulated miRNAs.

These and additional molecules function to block signal transduction in various pathways such that their down-regulation – potentially via miRNAs – will enhance signaling.

3.3. Differential DNA methylation and interaction with differential miRNA and mRNA in non-classical monocytes

Another important epigenetic mechanism of gene regulation is the control of gene expression via methylation of CpG sites in the vicinity of coding sequences. We therefore have determined the methylation status of the three monocyte subsets using methyl-seq (Zawada et al., 2016). Looking at non-classical monocytes as compared to both classical and intermediate cells, we found unique differential methylation (1.2-fold and probability > 0.8) for 4484 sites (see Table 2).

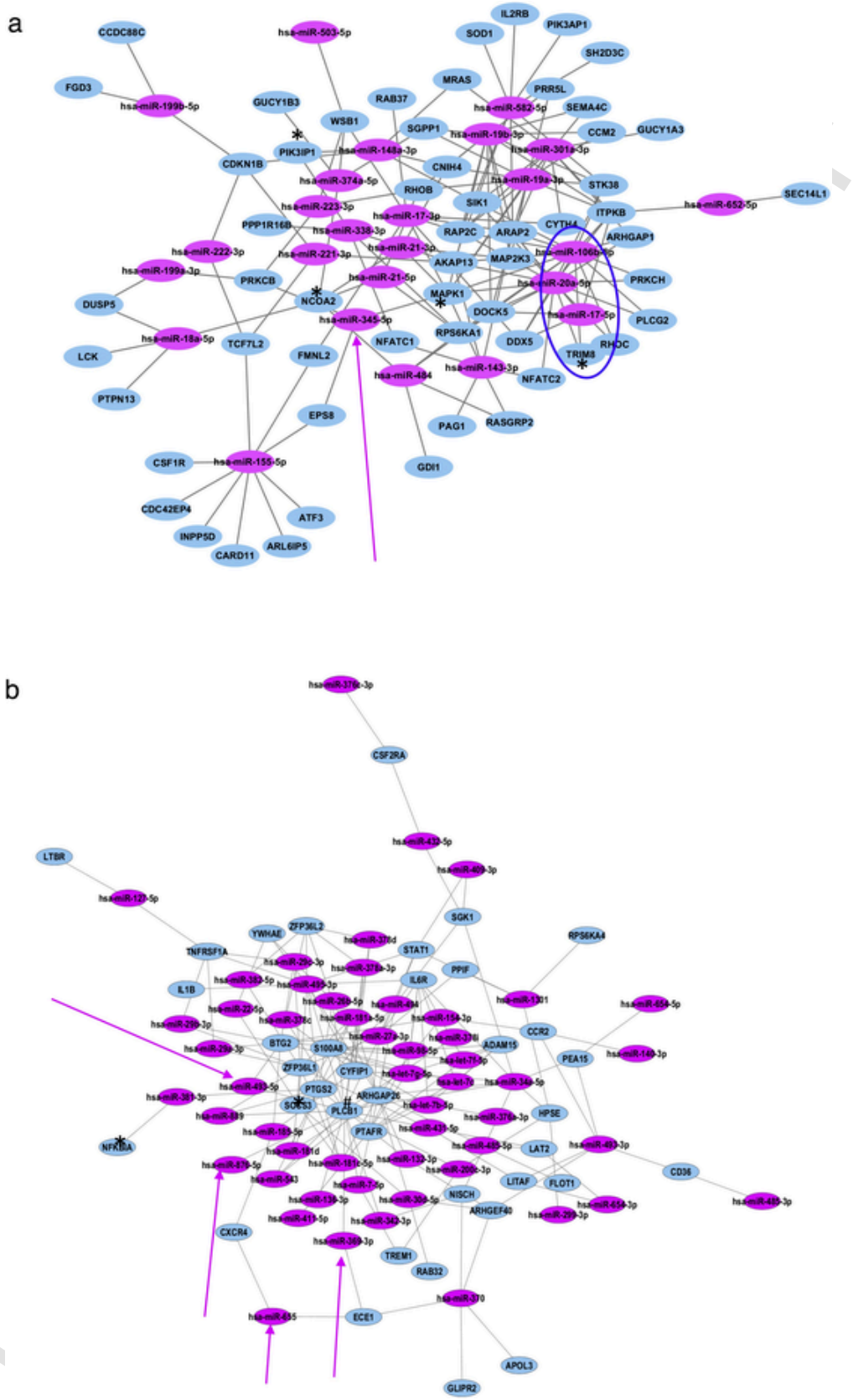

Fig. 3. Interaction of reciprocally regulated miRNA and mRNA for the subset of signaling associated mRNAs.(A) down-regulated miRNAs and up-regulated mRNAs, only the subset of 57 signaling associated mRNAs and their interacting miRNAs is shown, the full interaction map is given in Fig S1A. The arrow marks the top down-regulated miRNA. Up-regulated signaling

molecules that interact with down-regulated miRNAs include MAPK1(*), which is targeted by six miRNAs including the top down-regulated miRNA 345-5p, NCOA2 (*), which is targeted by five miRNAs, PI3KIP (*) targeted by two miRNAs and TRIM8, targeted by two miRNAs, i.e. miRNA-20a-5p and miRNA-106b-5p.(B) up-regulated miRNAs and down-regulated mRNAs, only the subset of 37 signaling associated mRNAs and their interacting miRNAs is shown, (the full interaction map is given in Fig S1B).The arrows mark the top up-regulated miRNAs. Many of the down-regulated mRNAs code for proteins that can block signal transduction. The asterisk (*) marks some typical examples like NFKBIA targeted by one miRNA and SOCS3 targeted by 5 miRNAs. # PLCB1, a molecule that promotes signaling.

Table 2
Differential DNA methylation in non-classical monocytes.

#loci	Total	upstream CpG	upstream CpG linked to DEGs	upstream CpG linked to DE miRs	upstream CpG linked to DE miRs that are linked to DEGs
Hypomethylated	4455	760	16	1	0
Hypermethylated	29	1	0	0	0

Most of these (n = 4455) were selectively hypo-methylated in non-classical monocytes and of these 760 are up-stream of mRNA coding genes. Analysis of biological processes for these mRNA only provided three general terms that were significant, i.e. cell development, organ development and stem cell development. We then asked whether these 760 hypo-methylated sites in non-classical monocytes go along with an increased gene expression in non-classical monocytes. We, in fact, found 16 sites that are linked to 14 selectively increased mRNA levels in non-classical monocytes (see Table 3).

The number of linked DEGs is lower because there are two genes, i.e. FGFRL1 and TRIM8, linked to two hypo-methylated sites each.

In addition, we found 80 hypo-methylated sites that are upstream of a miRNA gene but only one of these was linked to a differentially expressed miRNA (Table 2). The locus is chr8:135844258–135844263 and it is linked to hsa-miR-30d-5p, which is up-regulated in non-classical monocyte. This miRNA is not linked to a DEG. Hence, there was no hypo-methylated CpG upstream of an up-regulated miRNA that is linked to a reduced DEG.

We then asked whether among the genes, which are selectively hypo-methylated in the upstream region, there are genes that at the same time are targeted by a miRNA, which is down regulated in non-classical monocytes. In fact, we found 9 such differentially expressed genes (see Table 3). This includes genes involved in specific processes like fibroblast growth factor production and transforming growth factor beta-receptor signaling. Of note, TRIM8 is among these genes and it has two up-stream hypo-methylated sites (chr10:104402916–104402921 chr10:104403361–104403366) and it is targeted by two down-regulated miRNAs (20a-5p, 106b-5p).

3.4. Validation of the miRNA-20a / miRNA-106b -- TRIM8 -- TNF cascade

TRIM8 is a signaling molecule that positively feeds into the NF-κB pathway and can promote production of the pro-inflammatory cytokine tumor necrosis factor (TNF) (Versteeg et al., 2013). The levels for the two miRNAs, for TRIM8 mRNA and for TNF mRNA as obtained by sequencing in the present study is depicted in Figure S2 and this shows the pronounced decrease of the miRNAs, the increase of TRIM8 and the higher level of TNF mRNA in the non-classical monocytes.

In order to validate the findings of these analyses we have looked at a fresh set of classical and non-classical monocytes and have studied the 20a-5p and 106b-5p miRNAs, TRIM8 and TNF mRNAs by RT-PCR. Since cytokine levels are biologically most relevant after their expression has been induced by activation, we have looked at the patterns after LPS stimulation of classical and non-classical monocytes. For this, we have defined the non-classical monocytes via the slan marker, a cell surface molecule that has emerged as valuable tool to specifically define non-classical monocytes (Hofer et al., 2015).

When purified slan – CD16– classical and slan + CD16 + non-classical monocytes (Fig. 4) were incubated for 2 h without stimulation, then we noted lower miRNA-20a-5p and miRNA-106b-5p and higher TRIM8-mRNA and TNF-mRNA in the slan + non-classical monocytes compared to classical monocytes consistent with the findings for monocyte subsets defined via CD14 and CD16 only (Fig. 5).

With LPS stimulation (10 ng/mL) there was a trend towards a further decrease for the miRNAs and levels for both 20a-5p and 106b-5p remained significantly lower in non-classical monocytes. TRIM8 showed a slight decrease with LPS stimulation and there was a strong 10-fold increase in TNF mRNA expression with the level for non-classical monocytes being 6-times higher compared to classical monocytes. These data show that the pattern of decreased miRNAs and increased TRIM8 and TNF holds true when slan-defined monocyte subsets are stimulated with the TLR4 ligand LPS. Our data indicate that the signaling scheme that includes the action of miRNA-106b and -20a (Fig. 5) also applies to non-classical monocytes that are defined via slan.

4. Discussion

The discovery of monocyte subsets using flow cytometry dates back to the 1980s, when a CD16-positive and a CD16-negative monocyte was defined (Passlick et al., 1989). Later on an intermediate type of cell with a phenotype in between the two subsets was defined and was officially recognized (Ziegler-Heitbrock et al., 2010). In this study we have isolated the three subsets – classical, intermediate and non-classical monocytes – using the traditional CD14 and CD16 markers, but in addition we employed the slan-marker for more precise definition of non-classical monocytes. The slan marker, a 6-sulfo LacNAc carbohydrate residue coupled to the PSGL-1 cell surface molecule, was originally described as a marker for dendritic cells (DCs) (Schakel et al., 1998). However, early on it was noted that this molecule is expressed by CD16-positive monocytes and also by alveolar macrophages (Siedlar et al., 2000). Moreover, many characteristics reported for cells called slan + DCs were similar to CD16-positive monocytes. This includes high TNF production (Belge et al., 2002; Schakel et al., 2006), low IL-10 production (Frankenberger et al., 1996; de Baey et al., 2003) and the selective depletion by glucocorticoids (Fingerle-Rowson et al., 1998; Thomas et al., 2014). Duterte et al. have noted a strong increase of both non-classical monocytes and slan positive cells in HIV patient blood and have confirmed that slan is expressed on monocytes (Dutertre et al., 2012). More recently we have shown that the slan-positive cells have a unique gene expression pattern, which clusters with monocytes and not with DCs (Hofer et al, 2015). This has been further elaborated and consolidated by adding a comparison to CD141 DCs and by demonstrating a unique complement signature (van Leeuwen-Kerkhoff et al., 2017). Hence, slan has been established as a marker for definition of slan + CD16 + non-classical monocytes (Hofer et al., 2019).

The mechanisms leading to higher TNF production in non-classical monocytes are still elusive. Here, Ong et al. (2018) have shown higher protein levels for p65 of NF-κB in whole cell lysates of non-classical monocytes. p65 is part of the p50/p65 heterodimer, which is triggered by a signaling cascade that can be initiated by binding of lipopolysaccharide to the TLR4 receptor complex (Fig. 6). Higher levels of p65 in the cytoplasm indicate that there is a higher capacity to respond to upstream signals. We have looked into miRNAs as regulators of this upstream signaling cascade.

Earlier studies have looked at miRNA expression in CD16 + and CD16- monocyte subsets (Etzrodt et al., 2012; Bidzhekov et al.,

Table 3
Differentially upregulated genes with up-stream hypomethylated CpG sites and targeted or not by downregulated miRNAs.

Gene symbol	Ensembl ID	Gene name	Up-stream hypomethylated site	Hypo-methylation level (NLM)			miRNA targeting this mRNA	mRNA expression level (TPM)			Gene function
				Classical	Intermediate	Non-classical		Classical	Intermediate	Non-classical	
ANKH	ENSG00000154122	Progressive ankylosis homolog inorg anic pyrophosphate transport regulator	chr5:14872440–14872445	0.50	0.26	1.84	hsa-miR-143–3p, hsa-miR-223–3p, hsa-miR-20a-5p, hsa-miR-106b-5p	21	35	55	GO:0007626~locomotory behavior
KIAA1033	ENSG00000136051	WASH complex subunit 4	chr12:105501456–105501461	0.67	0.52	2.42	hsa-miR-20a-5p, hsa-miR-582-5p, hsa-miR-106b-5p, hsa-miR-143–3p, hsa-miR-155-5p, hsa-miR-19b-3p, hsa-miR-301a-3p, hsa-miR-484, hsa-miR-503-5p, hsa-miR-374a-5p, hsa-miR-19a-3p	113	113	155	GO:0016197~endosomal transport
CDH23	ENSG00000107736	Cadherin-related 23	chr10:73156498–73156503	0.96	0.52	2.31		54	173	259	GO:0007156~homophilic cell adhesion via plasma membrane adhesion molecules
CUX1	ENSG00000257923	Cut-like homeobox 1	chr7:101459131–101459136	0.67	0.61	2.36		198	499	1041	GO:0006357~regulation of transcription from RNA polymerase II promoter
FGFRL1	ENSG00000127418	Fibroblast growth factor receptor-like1	chr4:1003942–1003947 chr4:1004975–1004980	0.35 0.74	0.13 0.48	2.05 2.05		7	46	74	GO:0008543~fibroblast growth factor receptor signaling pathway
HEG1	ENSG00000173706	Heart development protein with EGF like domains	chr3:124774903–124774908	0.74	0.44	2.68	hsa-miR-20a-5p, hsa-miR-374a-5p, hsa-miR-301a-3p, hsa-miR-17-5p, hsa-miR-106b-5p, hsa-miR-345-5p	9	76	129	GO:0090271~positive regulation of fibroblast growth factor production,
INSIG1	ENSG00000186480	Insulin induced gene 1	chr7:155089286–155089291	1.98	2.36	5.52	hsa-miR-221–3p, hsa-miR-19b-3p, hsa-miR-19a-3p, hsa-miR-222–3p, hsa-miR-301a-3p	41	238	366	GO:0045717~negative regulation of fatty acid biosynthetic process
LNPEP	ENSG00000113441	Leucyl/cystinyl aminopeptidase	chr5:96270944–96270949	0.18	0.22	1.37	hsa-miR-223–3p, hsa-miR-301a-3p, hsa-miR-582-5p, hsa-miR-148a-3p, hsa-miR-374a-5p	78	109	155	GO:0042590~antigen processing and presentation of exogenous peptide antigen via MHC class I
LYST	ENSG00000143669	Lysosomal trafficking regulator	chr1:236030460–236030465	0.67	0.74	2.42	hsa-miR-223-3p, hsa-miR-19a-3p, hsa-miR-19b-3p	249	412	533	GO:0042742 ~defense response to bacterium, GO:0042832 ~defen se response to protozoan,GO:0051607~defense response to virus

Table 3 (*Continued*)

Gene symbol	Ensembl ID	Gene name	Up-stream hypomethylated site	Hypo-methylation level (NLM)			miRNA targeting this mRNA	mRNA expression level (TPM)			Gene function
				Classical	Intermediate	Non-classical		Classical	Intermediate	Non-classical	
PPDPF	ENSG00000125534	Pancreatic progenitor cell differentiation proliferation factor	chr20:62151706–62151711	0.39	0.22	1.47		233	296	419	GO:0001708~cell fate specification
SLC2A6	ENSG00000160326	Solute carrier family 2 member 6	chr9:136344380–136344385	1.56	1.75	4.10		74	179	264	GO:0046323~glucose import
SORT1	ENSG00000134243	Sortilin 1	chr1:109940798–109940803	1.03	0.13	2.78	hsa-miR-345-5p, hsa-miR-155-5p, hsa-miR-17-5p, hsa-miR-106b-5p, hsa-miR-20a-5p	123	139	175	GO:0046323~glucose import
TRIM8	ENSG00000171206	Tripartite motif containing 8	chr10:104402916–104402921 chr10:104403361–104403366	1.03 1.56	0.83 1.36	2.89 4.20	hsa-miR-20a-5p, hsa-miR-106b-5p	179	175	227	GO:0051092~positive regulation of NF-kappaB transcription factor, TRIM8, as a positive regulator of TNFα and IL-1β–triggered NF-κB activation. Li et al, PNAS, 2011,108:19341
ZNF703	ENSG00000183779	Zinc finger protein 703	chr8:37553095–37553100	1.20	1.75	4.04	hsa-miR-155-5p	38	228	285	GO:0017015~regulation of transforming growth factor beta receptor signaling pathway

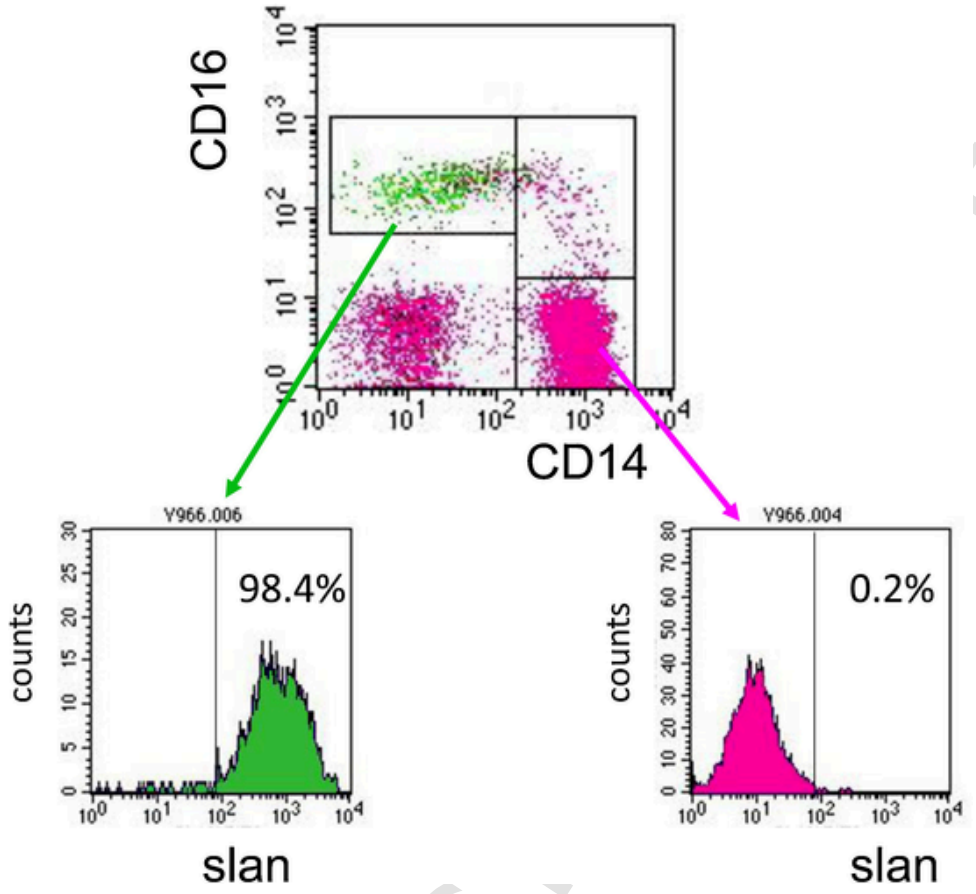

Fig. 4. Isolation of slan-defined non-classical and classical monocytes.Isolated blood mononuclear cells were stained with DR-APC, CD14-PC5, CD16 -PEand slan-FITC and at least 5.000 monocytes were analyzed by flow cytometry. The dot plot in the upper part of this experimental figure has also been used for illustration purposes in Hofer et al, Front. Immunol. 10:2052, doi 10.3389/fimmu.2019.02052. One representative sample of four.

2012; Dang et al., 2015). Etzrodt et al. noted 9 miRNAs with an at least 2-fold difference in expression in mouse classical and non-classical monocytes and the higher expression of miRNA-146a in mouse non-classical monocytes was confirmed for human CD16+ monocytes (Etzrodt et al., 2012). Bidzhekov et al. reported on a large number of differentially expressed miRNAs for human monocyte subsets with the strongest differences for miR-189, -147 and -1282 (high in CD16+ monocytes) and for miR-374a, -451 and -1225 (low in CD16+ monocytes) (Bidzhekov et al., 2012). Dang et al. found 66 differentially expressed miRNAs with an at least two-fold difference between CD16+ and CD16- subsets (Dang et al., 2015). Here the miRNAs with the strongest increase in CD16+ monocytes were miR-432, -212 and -409-3p and those with the strongest decrease were miR-19a, -345 and-452. The increase for miR-146a was also found, but none of the mentioned top miRNAs were shared between Dang et al. and Bidzhekov et al. When Duroux-Richard et al. (Duroux-Richard et al., 2019) have compared their own unpublished data with those of Dang et al., retrieved from the GEO data bank, they found a consistent differential expression in monocyte subsets for 9 miRNAs. Hence, there appears to be a large variability with respect to miRNAs differentially expressed between human monocyte subsets, which may be due to differences in cell preparation and in miRNA detection techniques used.

All of the above studies were done by comparing CD16+ monocytes and CD16- monocytes. However, as mentioned above, monocytes are currently subdivided into CD14++CD16− classical cells, CD14++CD16+ intermediate cells and CD14+CD16++ non-classical cells (Ziegler-Heitbrock et al., 2010). Therefore, in order to understand the mechanisms that specifically operate in non-classical monocytes, we have compared herein the CD14+CD16++ cells to both the intermediate and classical monocytes and we detected 92 miRNAs with an at least 2-fold difference as compared to both of the two other subsets. Given the more specific definition of the CD16+ non-classical monocytes and the additional comparison to the CD16+ intermediate monocytes, this is a high number of differential miRNAs. While several miRNAs from our study (e.g. top miR-493 and miRNA-345-5p and miR-146a) were also differential in the study by Dang et al. (Dang et al., 2015) we discovered many miRNAs not previously described in the context of monocyte subsets, i.e. more than 40 of our differential miRNAs were not found among the differential miRNAs described by Dang et al.(data not shown).

Biological processes linked to the differential miRNAs in previous studies were cell signaling (Etzrodt et al., 2012), chemotaxis and apoptosis (Dang et al., 2015) and monocyte differentiation (Selimoglu-Buet et al., 2018). The main biological process in our analysis turned out to be signaling (see Fig. 2A and B). Signaling molecules targeted in this context included NFKBIA, SOCS3, MAPK1, NCOA2 and TRIM8. Here, NFKBIA (also known as IKBalpha) and SOCS3 are known to block signaling pathways and these transcripts were downregulated. On the other hand, MAPK1, NCOA2 and TRIM8 are promoting signaling and their transcripts were up-regulated in non-classical monocytes. This indicates that miRNAs may serve to support gene expression in this monocyte subset by controlling expression of transcription factors. Given the higher TNF production in non-classical monocytes, we then focused on TRIM8, a positive regulator of NF-κB signal transduction. Here we have asked whether non-classical monocytes will maintain lower miRNA-106b and -20a and higher TRIM8 along with higher TNF

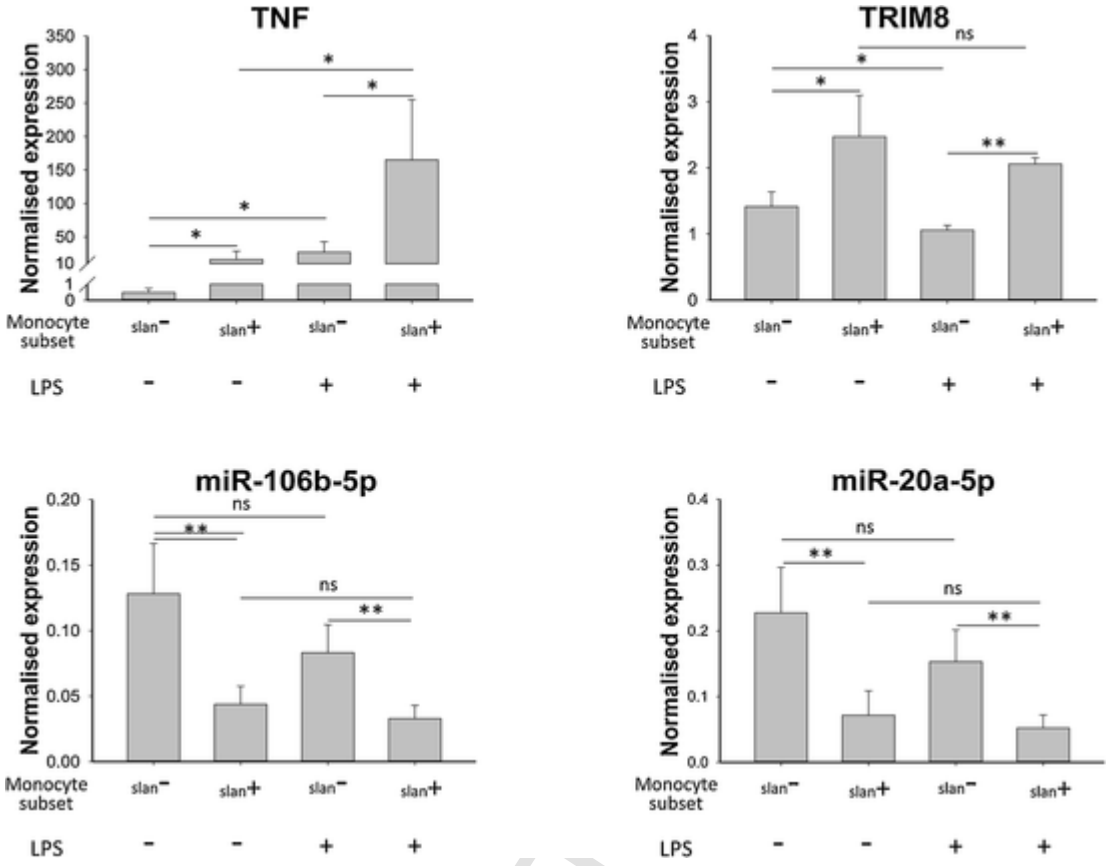

Fig. 5. miRNAs and down-stream TRIM8 and TNF in classical and non-classical monocytes defined via slan.Monocyte subsets were isolated using the slan marker. The slan-negative classical monocytes (slan−, also CD16−) and the slan-positive non-classical monocytes (slan+, also CD16+) with a purity > 90 %, were cultured for 2 h without and with LPS at 10 ng/mL. The mRNA and miRNA were isolated from lysates and was amplified by PCR. Results for normalized to SF3A1 for mRNAs and to RNU6-2 for miRNAs. $^{**}p < 0.01$, $^{*}p < 0.05$, ns = non-significant in Student's *t*-test. Mean ± SD of four experiments.

after TLR4 stimulation. In fact, LPS stimulated non-classical monocytes showed the predicted pattern and had significantly lower miRNA-106b and miRNA-20a and higher TRIM8 along with higher TNF compared to classical monocytes (see Fig. 5). This supports the concept of a signaling cascade that is controlled by these miRNAs and by TRIM8 in non-classical monocytes. The cartoon in Fig. 6 illustrates this signaling pathway. Here, low levels of miR-20a and -106b will allow for higher levels of TRIM8 such that it can support TAK1 action on IKK followed by mobilization of p50/p65 NF-kB into the nucleus and this promotes TNF gene expression.

Li et al. (Li et al., 2011) and Versteeg et al. (Versteeg et al., 2013) have shown that TRIM8 is a positive regulator of signal transduction and cytokine gene expression. On the other hand, studies in knock out animals suggested a negative role for TRIM8 in LPS induced gene expression in mice (Ye et al., 2017). While Ye et al. used germline knock-out in mice, which can entail compensatory mechanism in ontogeny, the work by Li et al. and Versteeg et al. were done with transfection in human cells. The work by Versteeg et al. (Versteeg et al., 2013) may be more relevant to our studies, which imply a positive role for TRIM8 in signal transduction. A positive impact of TRIM8 on cytokine expression was also shown in a recent study, which reported that TRIM8 is crucial to type I interferon production in human plasmacytoid DCs in that it protects the transcription factor IRF7 from proteasomal degradation (Maarifi et al., 2019). Therefore, the increased TRIM8 levels may impact on gene expression in non-classical monocytes beyond the TNF cytokine.

Regarding the epigenetic control of TRIM8 gene expression, miRNAs form one important component. In addition, methylation of CpG sites can repress gene expression and hypo-methylated promotors enable transcription (Weber et al., 2007; Greenberg and Bourc'his, 2019). When looking at differential methylation of CpG sites up-stream of mRNA coding genes, we noticed that there are two sites for the TRIM8 gene, which are hypo-methylated in non-classical monocytes. This may provide an additional mechanism for enhanced transcription of TRIM8 in non-classical monocytes.

As detailed above, the non-classical monocytes usually are dissected from intermediate monocytes based on their lower CD14 expression level. Since there is a gradual decrease of CD14 levels, the cut-off chosen is variable and different strategies have been tested (Zawada et al., 2015). Here, the use of additional markers for the dissection has been proposed (Wong et al., 2012). Therefore, we have now isolated non-classical monocytes as CD14+CD16+slan+ cells and classical monocytes as CD14++CD16-slan− cells and have studied the miRNAs, TRIM8 and TNF with and without LPS stimulation. Using this approach, we have shown herein that the mechanisms of epigenetic control of the high TNF production by the non-classical monocytes also apply to these cells when defined via slan.

Taken together our data provide evidence for pathways of epigenetic control of cytokine gene expression involving miRNAs and CpG methylation sites unique to non-classical monocytes.

Author's contribution

L.Z., T.P.H., A.M.Z. and B.K. have performed experiments, B.K. and N.K. curated the data and all authors analyzed these data, all authors contributed to the writing, L.Z.H. has developed the project and drafted the paper, all authors have approved the final version of the manuscript.

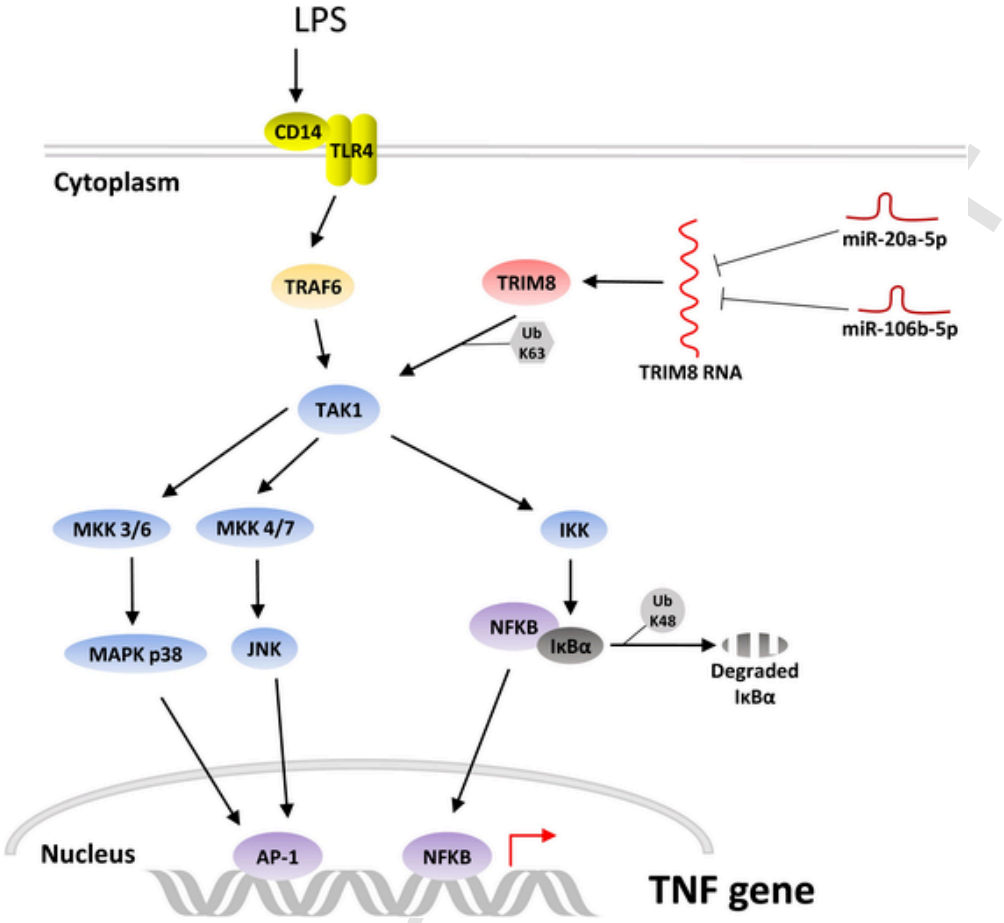

Fig. 6. Signaling scheme showing contribution of miRNA-20a-5p and miRNA 106b-5p to LPS induced TNF gene expression via TRIM8.The interaction of miR-20a-5p and 106b-5p with TRIM8 is based on HITS–CHIP data by Riley et al. (2012), see supplement Table S8 therein. The interaction of TRIM8 and TAK1 all the way down to JNK and AP1 was documented in Li et al. (2011), the regulation of JNK and p38 by TAK1 was reported by Chen et al. (2015) and the TAK1 IKK interaction was demonstrated in Sakurai et al. (1999). Ablation of TRIM8 by RNA interference was shown to lead to reduced expression of TNF by Versteeg et al. (2013). IKK will phosphorylate IkBa, which subsequently is degraded. This liberates the p50p65 NFκB complex that can move into the nucleus.

Declaration of Competing Interest

A.M.Z. is currently full-time employee of Fresenius Medical Care; the present work was performed and completed under the previous given affiliation (Saarland University Medical Center). All authors declare no conflict of interest.

Acknowledgments

Y.D. is funded by the National Research Fund (grants # C14/BM/8225223 and C17/BM/11613033), the Ministry of Higher Education and Research and the Heart Foundation–Daniel Wagner of Luxembourg.

Appendix A. Supplementary data

Supplementary material related to this article can be found, in the online version, at doi:https://doi.org/10.1016/j.imbio.2020.151958.

References

Anders, S, Huber, W, 2010. Differential expression analysis for sequence count data. Genome Biol. 11, R106.

Belge, K U, Dayyani, F, Horelt, A, Siedlar, M, Frankenberger, M, Frankenberger, B, Espevik, T, Ziegler-Heitbrock, L, 2002. The proinflammatory CD14+CD16+DR++ monocytes are a major source of TNF. J. Immunol. 168, 3536.

Bidzhekov, K, Gan, L, Denecke, B, Rostalsky, A, Hristov, M, Koeppel, T A, Zernecke, A, Weber, C, 2012. microRNA expression signatures and parallels between monocyte subsets and atherosclerotic plaque in humans. Thromb. Haemost. 107, 619.

Carbon, S, Ireland, A, Mungall, C J, Shu, S, Marshall, B, Lewis, S, Ami, G O H, Web Presence Working, G., 2009. AmiGO: online access to ontology and annotation data. Bioinformatics 25, 288.

Chen, I T, Hsu, P H, Hsu, W C, Chen, N J, Tseng, P H, 2015. Polyubiquitination of transforming growth factor beta-activated kinase 1 (TAK1) at lysine 562 residue regulates TLR4-mediated JNK and p38 MAPK activation. Sci. Rep. 5, 12300.

Dang, T M, Wong, W C, Ong, S M, Li, P, Lum, J, Chen, J, Poidinger, M, Zolezzi, F, Wong, S C, 2015. MicroRNA expression profiling of human blood monocyte subsets highlights functional differences. Immunology 145, 404.

Dayyani, F, Belge, K U, Frankenberger, M, Mack, M, Berki, T, Ziegler-Heitbrock, L, 2003. Mechanism of glucocorticoid-induced depletion of human CD14+CD16+ monocytes. J. Leukoc. Biol. 74, 33.

de Baey, A, Mende, I, Baretton, G, Greiner, A, Hartl, W H, Baeuerle, P A, Diepolder, H M, 2003. A subset of human dendritic cells in the T cell area of mucosa-associated lymphoid tissue with a high potential to produce TNF-alpha. J. Immunol. 170, 5089.

de Hoon, M J, Imoto, S, Nolan, J, Miyano, S, 2004. Open source clustering software. Bioinformatics 20, 1453.

Duroux-Richard, I, Robin, M, Peillex, C, Apparailly, F, 2019. MicroRNAs: fine tuners of monocyte heterogeneity. Front. Immunol. 10, 2145.

Dutertre, C A, Amraoui, S, DeRosa, A, Jourdain, J P, Vimeux, L, Goguet, M, Degrelle, S, Feuillet, V, Liovat, A S, Muller-Trutwin, M, Decroix, N, Deveau, C, Meyer, L, Goujard, C, Loulergue, P, Launay, O, Richard, Y, Hosmalin, A, 2012. Pivotal role of M-DC8(+) monocytes from viremic HIV-infected patients in TNFalpha overproduction in response to microbial products. Blood 120, 2259.

Etzrodt, M, Cortez-Retamozo, V, Newton, A, Zhao, J, Ng, A, Wildgruber, M, Romero, P, Wurdinger, T, Xavier, R, Geissmann, F, Meylan, E, Nahrendorf, M, Swirski, F K, Baltimore, D, Weissleder, R, Pittet, M J, 2012. Regulation of monocyte functional heterogeneity by miR-146a and Relb. Cell Rep. 1, 317.

Fingerle, G, Pforte, A, Passlick, B, Blumenstein, M, Strobel, M, Ziegler-Heitbrock, H W, 1993. The novel subset of CD14+/CD16+ blood monocytes is expanded in sepsis patients. Blood 82, 3170.

Fingerle-Rowson, G, Angstwurm, M, Andreesen, R, Ziegler-Heitbrock, H W, 1998. Selective depletion of CD14+ CD16+ monocytes by glucocorticoid therapy. Clin. Exp. Immunol. 112, 501.

Frankenberger, M, Sternsdorf, T, Pechumer, H, Pforte, A, Ziegler-Heitbrock, H W, 1996. Differential cytokine expression in human blood monocyte subpopulations: a polymerase chain reaction analysis. Blood 87, 373.

Greenberg, M V C, Bourc'his, D, 2019. The diverse roles of DNA methylation in mammalian development and disease. Nat. Rev. Mol. Cell Biol. 20, 590.

Hochberg, Y, 1988. A sharper Bonferroni procedure for multiple tests of significance. Biometrika 75, 800.

Hofer, T P, Zawada, A M, Frankenberger, M, Skokann, K, Satzl, A A, Gesierich, W, Schuberth, M, Levin, J, Danek, A, Rotter, B, Heine, G H, Ziegler-Heitbrock, L, 2015. Slan-defined subsets of CD16-positive monocytes: impact of granulomatous inflammation and M-CSF receptor mutation. Blood 126, 2601.

Hofer, T P, van de Loosdrecht, A A, Stahl-Hennig, C, Cassatella, M A, Ziegler-Heitbrock, L, 2019. 6-Sulfo LacNAc (slan) as a marker for non-classical monocytes. Front. Immunol. 10, 2052.

Huang da, W, Sherman, B T, Lempicki, R A, 2009. Systematic and integrative analysis of large gene lists using DAVID bioinformatics resources. Nat. Protoc. 4, 44.

Li, Q, Yan, J, Mao, A P, Li, C, Ran, Y, Shu, H B, Wang, Y Y, 2011. Tripartite motif 8 (TRIM8) modulates TNFalpha- and IL-1beta-triggered NF-kappaB activation by targeting TAK1 for K63-linked polyubiquitination. Proc. Natl. Acad. Sci. U.S.A. 108, 19341.

Maarifi, G, Smith, N, Maillet, S, Moncorge, O, Chamontin, C, Edouard, J, Sohm, F, Blanchet, F P, Herbeuval, J P, Lutfalla, G, Levraud, J P, Arhel, N J, Nisole, S, 2019. TRIM8 is required for virus-induced IFN response in human plasmacytoid dendritic cells. Sci. Adv. 5 eaax3511.

Muller, S, Rycak, L, Winter, P, Kahl, G, Koch, I, Rotter, B, 2013. omiRas: a Web server for differential expression analysis of miRNAs derived from small RNA-Seq data. Bioinformatics 29, 2651.

Ong, S M, Hadadi, E, Dang, T M, Yeap, W H, Tan, C T, Ng, T P, Larbi, A, Wong, S C, 2018. The pro-inflammatory phenotype of the human non-classical monocyte subset is attributed to senescence. Cell Death Dis. 9, 266.

Paraskevopoulou, M D, Georgakilas, G, Kostoulas, N, Vlachos, I S, Vergoulis, T, Reczko, M, Filippidis, C, Dalamagas, T, Hatzigeorgiou, A G, 2013. DIANA-microT web server v5.0: service integration into miRNA functional analysis workflows. Nucleic Acids Res. 41, W169.

Passlick, B, Flieger, D, Ziegler-Heitbrock, H W, 1989. Identification and characterization of a novel monocyte subpopulation in human peripheral blood. Blood 74, 2527.

Riley, K J, Rabinowitz, G S, Yario, T A, Luna, J M, Darnell, R B, Steitz, J A, 2012. EBV and human microRNAs co-target oncogenic and apoptotic viral and human genes during latency. EMBO J. 31, 2207.

Rogacev, K S, Cremers, B, Zawada, A M, Seiler, S, Binder, N, Ege, P, Grosse-Dunker, G, Heisel, I, Hornof, F, Jeken, J, Rebling, N M, Ulrich, C, Scheller, B, Bohm, M, Fliser, D, Heine, G H, 2012. CD14++CD16+ monocytes independently predict cardiovascular events: a cohort study of 951 patients referred for elective coronary angiography. J. Am. Coll. Cardiol. 60, 1512.

Sakurai, H, Miyoshi, H, Toriumi, W, Sugita, T, 1999. Functional interactions of transforming growth factor beta-activated kinase 1 with IkappaB kinases to stimulate NF-kappaB activation. J. Biol. Chem. 274, 10641.

Saldanha, A J, 2004. Java Treeview--extensible visualization of microarray data. Bioinformatics 20, 3246.

Schakel, K, Mayer, E, Federle, C, Schmitz, M, Riethmuller, G, Rieber, E P, 1998. A novel dendritic cell population in human blood: one-step immunomagnetic isolation by a specific mAb (M-DC8) and in vitro priming of cytotoxic T lymphocytes. Eur. J. Immunol. 28, 4084.

Schakel, K, Kannagi, R, Kniep, B, Goto, Y, Mitsuoka, C, Zwirner, J, Soruri, A, von Kietzell, M, Rieber, E, 2002. 6-Sulfo LacNAc, a novel carbohydrate modification of PSGL-1, defines an inflammatory type of human dendritic cells. Immunity 17, 289.

Schakel, K, von Kietzell, M, Hansel, A, Ebling, A, Schulze, L, Haase, M, Semmler, C, Sarfati, M, Barclay, A N, Randolph, G J, Meurer, M, Rieber, E P, 2006. Human 6-sulfo LacNAc-expressing dendritic cells are principal producers of early interleukin-12 and are controlled by erythrocytes. Immunity 24, 767.

Selimoglu-Buet, D, Riviere, J, Ghamlouch, H, Bencheikh, L, Lacout, C, Morabito, M, Diop, M, Meurice, G, Breckler, M, Chauveau, A, Debord, C, Debeurme, F, Itzykson, R, Chapuis, N, Willekens, C, Wagner-Ballon, O, Bernard, O A, Droin, N, Solary, E, 2018. A miR-150/TET3 pathway regulates the generation of mouse and human non-classical monocyte subset. Nat. Commun. 9, 5455.

Shannon, P, Markiel, A, Ozier, O, Baliga, N S, Wang, J T, Ramage, D, Amin, N, Schwikowski, B, Ideker, T, 2003. Cytoscape: a software environment for integrated models of biomolecular interaction networks. Genome Res. 13, 2498.

Siedlar, M, Frankenberger, M, Ziegler-Heitbrock, L H, Belge, K U, 2000. The M-DC8-positive leukocytes are a subpopulation of the CD14+ CD16+ monocytes. Immunobiology 202, 11.

Tarazona, S, Garcia-Alcalde, F, Dopazo, J, Ferrer, A, Conesa, A, 2011. Differential expression in RNA-seq: a matter of depth. Genome Res. 21, 2213.

Thomas, K, Dietze, K, Wehner, R, Metz, I, Tumani, H, Schultheiss, T, Gunther, C, Schakel, K, Reichmann, H, Bruck, W, Schmitz, M, Ziemssen, T, 2014. Accumulation and therapeutic modulation of 6-sulfo LacNAc(+) dendritic cells in multiple sclerosis. Neurol. Neuroimmunol. Neuroinflamm. 1, e33.

van Leeuwen-Kerkhoff, N, Lundberg, K, Westers, T M, Kordasti, S, Bontkes, H J, de Gruijl, T D, Lindstedt, M, van de Loosdrecht, A A, 2017. Transcriptional profiling reveals functional dichotomy between human slan(+) non-classical monocytes and myeloid dendritic cells. J. Leukoc. Biol. 102, 1055.

Versteeg, G A, Rajsbaum, R, Sanchez-Aparicio, M T, Maestre, A M, Valdiviezo, J, Shi, M, Inn, K S, Fernandez-Sesma, A, Jung, J, Garcia-Sastre, A, 2013. The E3-ligase TRIM family of proteins regulates signaling pathways triggered by innate immune pattern-recognition receptors. Immunity 38, 384.

Vlachos, I S, Zagganas, K, Paraskevopoulou, M D, Georgakilas, G, Karagkouni, D, Vergoulis, T, Dalamagas, T, Hatzigeorgiou, A G, 2015. DIANA-miRPath v3.0: deciphering microRNA function with experimental support. Nucleic Acids Res. 43, W460.

Wang, L, Feng, Z, Wang, X, Wang, X, Zhang, X, 2010. DEGseq: an R package for identifying differentially expressed genes from RNA-seq data. Bioinformatics 26, 136.

Weber, M, Hellmann, I, Stadler, M B, Ramos, L, Paabo, S, Rebhan, M, Schubeler, D, 2007. Distribution, silencing potential and evolutionary impact of promoter DNA methylation in the human genome. Nat. Genet. 39, 457.

Wong, K L, Tai, J J, Wong, W C, Han, H, Sem, X, Yeap, W H, Kourilsky, P, Wong, S C, 2011. Gene expression profiling reveals the defining features of the classical, intermediate, and nonclassical human monocyte subsets. Blood 118, e16.

Wong, K L, Yeap, W H, Tai, J J, Ong, S M, Dang, T M, Wong, S C, 2012. The three human monocyte subsets: implications for health and disease. Immunol. Res. 53, 41.

Ye, W, Hu, M M, Lei, C Q, Zhou, Q, Lin, H, Sun, M S, Shu, H B, 2017. TRIM8 negatively regulates TLR3/4-Mediated innate immune response by blocking TRIF-TBK1 interaction. J. Immunol. 199, 1856.

Zawada, A M, Rogacev, K S, Rotter, B, Winter, P, Marell, R R, Fliser, D, Heine, G H, 2011. SuperSAGE evidence for CD14++CD16+ monocytes as a third monocyte subset. Blood 118, e50.

Zawada, A M, Fell, L H, Untersteller, K, Seiler, S, Rogacev, K S, Fliser, D, Ziegler-Heitbrock, L, Heine, G H, 2015. Comparison of two different strategies for human monocyte subsets gating within the large-scale prospective CARE FOR HOMe Study. Cytometry A 87, 750.

Zawada, A M, Schneider, J S, Michel, A I, Rogacev, K S, Hummel, B, Krezdorn, N, Muller, S, Rotter, B, Winter, P, Obeid, R, Geisel, J, Fliser, D, Heine, G H, 2016. DNA methylation profiling reveals differences in the 3 human monocyte subsets and identifies uremia to induce DNA methylation changes during differentiation. Epigenetics 11, 259.

Zawada, A M, Zhang, L, Emrich, I E, Rogacev, K S, Krezdorn, N, Rotter, B, Fliser, D, Devaux, Y, Ziegler-Heitbrock, L, Heine, G H, 2017. MicroRNA profiling of human intermediate monocytes. Immunobiology 222, 587.

Ziegler-Heitbrock, L, Ancuta, P, Crowe, S, Dalod, M, Grau, V, Hart, D N, Leenen, P J, Liu, Y J, MacPherson, G, Randolph, G J, Scherberich, J, Schmitz, J, Shortman, K, Sozzani, S, Strobl, H, Zembala, M, Austyn, J M, Lutz, M B, 2010. Nomenclature of monocytes and dendritic cells in blood. Blood 116, e74.